International Journal of Pavement Research and Technology
https://doi.org/10.1007/s42947-023-00349-0

社團法人中華鋪面工程學會
Chinese Society of Pavement Engineering

ORIGINAL RESEARCH PAPER

Performance of Soft Computing Technique in Predicting the Pavement International Roughness Index: Case Study

Abdualmtalab Abdualaziz Ali[1,2] · **Amgad Hussein**[1] · **Usama Heneash**[3]

Received: 23 June 2022 / Revised: 17 November 2022 / Accepted: 10 June 2023

Abstract
The International Roughness Index (IRI) is the most popular index used to measure road surface roughness. In the current study, three integrated approaches based on Multiple Linear Regression (MLR), Artificial Neural Networks (ANNs), and Fuzzy Inference System (FIS) techniques were conducted to develop linear and nonlinear regression models using IRI and pavement distress parameters. The pavement distress data were collected on 19 roads in the St. John's road network in Newfoundland, Canada, using a network "TotalPave" application. Several significant variables related to surface pavement distress were included as input parameters to develop the correlation between the IRI and pavement distress variables; eight input parameters included rutting, fatigue cracking, block cracking, longitudinal cracking, transverse cracking, potholes, patching, and delamination. The performance of the three techniques used in this study was evaluated using the coefficient of determination (R^2), Root Mean Squared Error (RMSE), and Mean Absolute Error (MAE). The results of the models revealed that the MLR, ANN, and FIS models could accurately predict IRI. According to ANNs, a coefficient of determination indicated that the correlation was increased by 60.7%, 46.5%, 12.34% and 11.01%. While RMSE was reduced by 73.6%, 78.7%, 51.32%, 70.4%, and MAE was reduced by 71.7%, 73.6%, 47.5%, and 61.1% compared to MLR and FIS, respectively. As a result, the ANN model indicated a better prediction of IRI for a given set of pavement distress parameters than FIS and MLR techniques.

Keywords Artificial neural network · Fuzzy Inference Index (FIS) · International Roughness Index (IRI) · Pavement performance · Multiple Linear Regression (MLR)

1 Introduction

Pavement performance and evaluation are essential for Pavement Management Systems (PMS). The condition and functional changes of pavements as they age are referred to as pavement performance [1]. In other words, the ability of pavements to withstand traffic intensity and climatic conditions, functionally and structurally, can be used to assess performance. Pavement structural failure occurs as a result of stresses caused by heavy traffic. When pavements fail to provide a smooth riding surface, this is referred to as functional failure. Uneven pavement causes discomfort for drivers and passengers and raises vehicle operating costs [2].

Several factors can be used to assess the condition and serviceability of pavements, including the Present Serviceability Index (PSI), the Pavement Condition Index (PCI), and the International Roughness Index (IRI). IRI, in particular, is a primary performance measure that highway agencies frequently use to forecast pavement performance. The current study aims to use field survey data to develop IRI prediction modelling using Multiple Linear Regression (MLR), Artificial Neural Network (ANN) and Fuzzy Inference Index (FIS) techniques. The IRI was created to provide a standardized global measurement for comparing pavement roughness. The average rectified slope (accumulated suspension motion to distance travelled) derived from a mathematical model of a standard quarter car passing over a measured profile at 80.5 km/h is defined as the IRI of pavement [3, 4]. The roughness or smoothness of the pavement

✉ Abdualmtalab Abdualaziz Ali
aayali@mun.ca; aayali@azu.edu.ly

Amgad Hussein
ahussein@mun.ca

Usama Heneash
usama.heneash@eng.kfa.edu.eg

[1] Memorial University, St. John's, Canada

[2] Azzaytuna University, Tarhuna, Libya

[3] Kafr El Sheikh University, Kafr El Sheikh, Egypt

Published online: 03 July 2023

is a comprehensive assessment indicator that considers the ride quality, comfort of the pavement and the presence of collective distresses. The IRI of the pavement increases as it ages, indicating deterioration.

Several techniques were used for pavement performance modelling, such as multiple linear regression, ANN, and fuzzy logic. ANN for modelling infrastructure deterioration are becoming more popular, and numerous studies have been conducted to evaluate their effectiveness.

According to the U.S. Department of Transportation, pavement ride quality based on IRI can be categorized into five groups, as shown in Table 1 [5].

2 Literature Review

2.1 Multiple Linear Regression

MLR is commonly used to investigate the relationship between input and output variables. A traditional regression method is a comprehensive tool for analyzing input and output parameters' relationships. Linear regression is one of the most commonly used statistical techniques [6]. The following equation gives the traditional linear regression model:

$$Y = C + a_1X_1 + a_2X_2 + \ldots\ldots\ldots\ldots\ldots\cdots + a_nX_n, \quad (1)$$

where Y is the dependent variable, C is the constant, X is the $(x_1,x_2,\ldots,x_n)$ independent variable, and $a_1, a_2, a_3 \ldots\ldots\ldots\ldots a_n$= coefficients.

According to Okine et al. [7], a technique for IRI prediction using Multivariate Adaptive Regression Splines (MARS) allowed them to determine the relative importance of pavement conditions, traffic, and environmental parameters.

Choi et al. [8] used the MLR method to predict the IRI model based on asphalt concrete properties. The model considered Asphalt Concrete (AC), the percent passing no 200 seize (P200) as input factors. According to Wang et al. [9], the Mechanistic-Empirical Pavement Design Guide employs IRI as a primary mode of assessing pavement condition and as one of the primary functional performance indicators (MEPDG).

Owolabi et al. [10] used the MLR method to predict performance models. The models took into account the input factors of fatigue cracking, longitudinal cracks, patching, potholes, and rut depth. The MLR method was used by Khattak et al. [11] to develop IRI models for hot mix asphalt.

Mubaraki [12] investigated the relationship between IRI and pavement damage on the highway connecting Jeddah and Jazan in Saudi Arabia. The study's findings revealed a significant relationship between IRI and cracking and IRI and ravelling. The results also show that rutting has no significant association with IRI values.

2.2 Artificial Neural Network (ANN)

ANNs are recent computational models defined in analogy with biological characteristics to simulate the decision process in the brain. This technique helps approximate and estimate unknown functions depending on various and numerous input values. One of the most important characteristics of this method is that it represents a method for solving extremely complex and nonlinear problems using only a few simple mathematical operations [13].

Machine Learning (ML) techniques are one of the most important methods for predicting pavement performance indicators. Chen et al. [14] genetic algorithms programming, gray forecast, and multiple regression are helpful tools for predicting IRI distress.

According to Hoang et al. [15, 16], seven methods of ML were used to investigate pavement distress, Naïve Bayesian Classifier (NBC), ANN, Random Forest (RF), Support Vector Machine (SVM), Radial Basis Function Neural Network (RBFNN), and Classification Tree (CT). Nabipour et al. [17] applied Genetic Expression Programming (GEP) and SVM techniques to predict the remaining service life pavement.

Ceylan et al. [18] published a study on ANN in pavement engineering. According to Terzi [19], predicting PSI with pavement distress is possible. Kirbaß and Karaßahin [20] studied ANN and MLR for calculating pavement performance models based on PCI. Platei et al. [21] used ANNs to assess pavement structural conditions based on FWD data. Other significant approaches to the study of compaction factors have been proposed in infrastructure engineering [22], evaluating drivers' perception of conditions [23], assessing

Table 1 Pavement ride quality based on roughness

Category	IRI rating (m/Km), by highway type		Interstate and noninterstate ride quality
	Interstate	Noninterstate	
Very good	< 1	< 1.0	Acceptable 0–2.0
Good	1.0–1.5	1.0–1.50	
Fair	1.5–1.90	1.50–2.70	
Poor	1.9–2.70	2.70–3.50	–
Very poor	> 2.70	> 3.5	Less than acceptable > 2.70

maintenance costs and prioritizing maintenance [24], and analyzing asphalt binders' ageing characteristics [25].

Amin MSR and Jiménez [26] published a case study of the Montreal road network. They considered simulated traffic over five decades. They also factored in the uncertainty of pavement performance in their calculations. They also used the backpropagation neural network (BPN) with the generalized delta rule learning algorithm, where uncertainties were ignored. Annual Average Daily Traffic (AADT), Equivalent Single Axle Loads (ESAL), and the pavement condition index were used to calculate the estimated PCI values. Marcelino et al. [27] applied the RF technique to predict IRI.

Vyas et al. [28] attempted to develop correlations using a variety of environmental structural, subgrade soil attributes, and functional inputs to estimate two different deflection basin parameters. The authors investigated a 124-km-long pavement network. They trained various ANN models with multiple architectures, each with one or more hidden layers. They compared the results of the ANN to those of MLR models and other intelligent techniques, and the ANN performed better than the other techniques.

Nitsche et al. [29] attempted to predict Weighted Longitudinal Profile (WLP) indices. Their goal was to assess the effectiveness of these techniques in estimating range and standard deviation.

Younos et al. [30] developed a pavement condition index prediction model that considers climatic parameters, pavement thickness, weighted plasticity index, and traffic loading. Linear regression and neural networks were the two methods utilized (ANN). The R^2 for the regression model was 0.80, while the R^2 for the ANN model was 0.88. Inkoom et al. [31] used various ML techniques, including bootstrap forest, gradient-boosted trees, K nearest neighbours, nave Bayes, and multiple linear regression.

Researchers proposed using a Multi-Stage Hyper-Heuristic (CMS-HH) approach to address specific combinatorial optimization issues, and they applied a self-learning discrete Jaya algorithm (SD-Jaya) to address the energy-efficient distributed no-idle Flow-shop Scheduling Problem (FSP) [32, 33].

A neural network is an interconnected group of artificial neurons that uses a connectionist approach to computation to process information. ANN is an adaptive system that changes its structure in response to external or internal information flowing through the network during the learning phase. Modern neural networks are tools for nonlinear statistical data modelling. They are used to model complex relationships between inputs and outputs and discover patterns in data. A series of layers typically represent them. Figure 1 shows that these layers usually consist of an input layer, several hidden layers, and an output layer. As shown in Fig. 1, each neuron in the ANN functions as a processing unit, the inputs are received, and the output is turned over to the next layer [34]. In each layer, neurons are connected to neurons in the next layer. Ann's nonlinear relationship

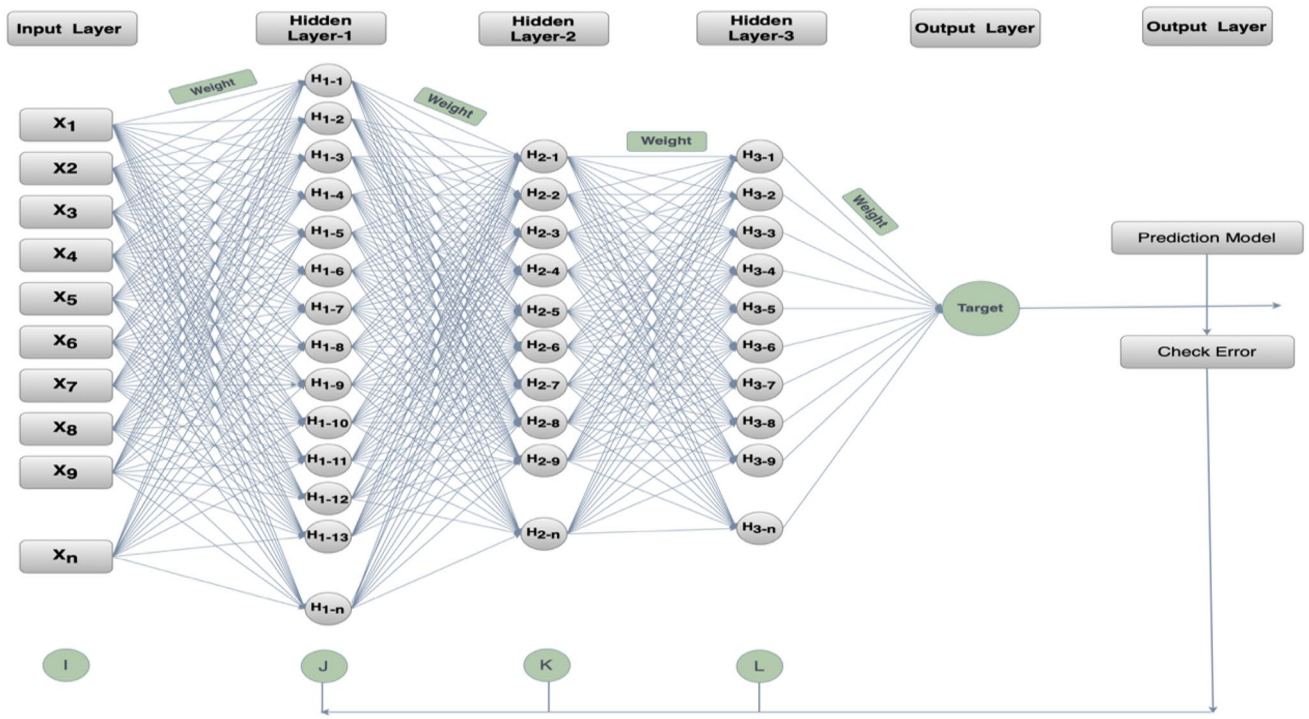

Fig. 1 Schematic representation of ANNs

between input and output layers requires a function to make a correlation between the neurons. Three transfer functions provide computation between neurons of different layers: Log-Sigmoid, Tan-Sigmoid, and Linear [35]. The following equations describe these functions:

$$\text{logsig}(x) = \frac{1}{1+e^{-x}}, \tag{2}$$

$$\text{tansig}(x) = \frac{2}{1+e^{-2x}} - 1, \tag{3}$$

$$\text{purelin}(x) = x. \tag{4}$$

The processing of each neuron is simply a weighted summation that is transferred via the activation function, as shown in Eq. (4).

$$Y_j = f\sum_{i=1}^{n} x_i w_{ij}, \tag{5}$$

where Y_j is the output of j the neuron, f is the activation function, n is the total number of inputs in this layer, x_i is i the input, and w_{ij} is the connection weight between ith input and the neuron.

2.3 Fuzzy Inference System (FIS)

The term "fuzzy" refers to a lack of clarity, and this fuzziness is caused by modelling the most similar human inference using a complex mathematical pattern. A fuzzy system converts human knowledge into mathematical formulas.

This critical activity uses linguistic variables, "if–then" fuzzy rules, and a mapping system (fuzzy engine). Knowledge and rules underpin fuzzy systems [36]. A fuzzy system's heart is a knowledge base comprised of fuzzy "if–then" rules. The first step in creating a fuzzy system is collecting a set of fuzzy "if–then" rules from expert knowledge or studying literature in the related field. The following step combines these rules into mathematical forms [37].

Fuzzy logic is one of the methods used in handling the uncertainties in the model or the data. FIS are based on fuzzy rules called fuzzy "if–then" rules. In some resources, instead of FIS, terms such as fuzzy model, fuzzy associative memory, and fuzzy logic controller are also used [38]. Fuzzy systems employ fuzzy sets to convert input variables to output variables [39]. These systems are especially useful for incorporating human experiences and behavioural data into the model. The model's variables are expressed in this way using fuzzy subsets. Fuzzy set operations are used for the inference under consideration. By generalizing classical set operations, these operations are obtained. A general fuzzy system has five layers, as shown in Fig. 2. The FIS structure has five layers, as follows:

2.3.1 Fuzzification Layer

This layer consists of defined membership functions of the input parameters. The result is a degree of membership value calculated using a Gaussian membership function [40].

$$\mu_{Ai}(x) = \exp\left[-\left(\frac{x-c_i}{2\delta_i^2}\right)^2\right], \tag{6}$$

where c_i, δ_i are parameters of a membership function.

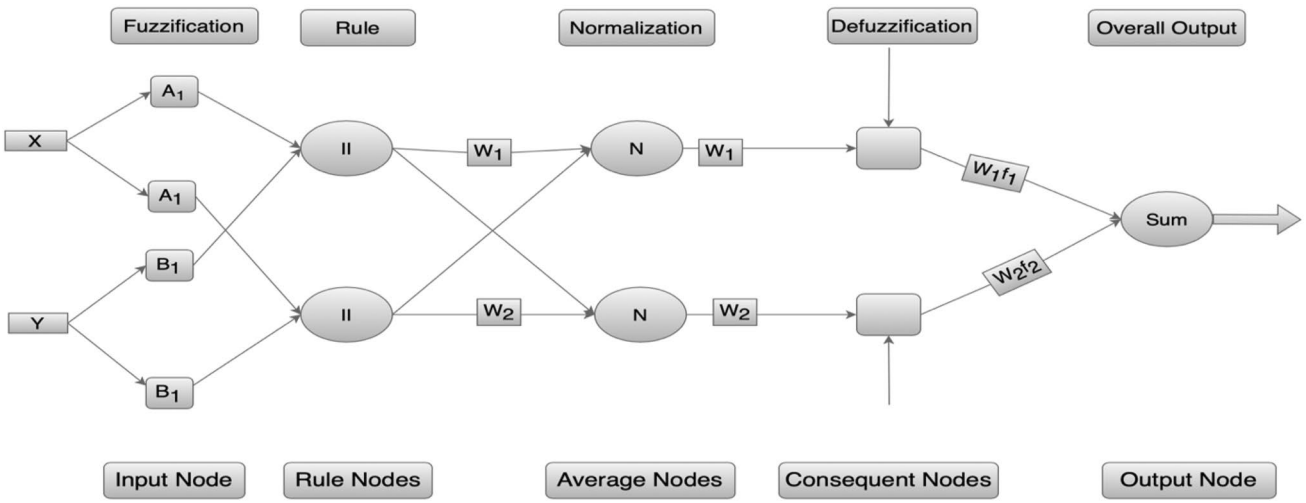

Fig. 2 Schematic representation of a fuzzy system

2.3.2 Rule Layer

This layer applies fuzzy AND to the previous part of the fuzzy rules.

$$\omega_i = \mu_{Ai}(x) * \mu_{Bi}(x). \tag{7}$$

2.3.3 Normalized Layer

This layer normalized the membership functions.

$$\overline{\omega_i} = \frac{\omega_i}{\sum_i \omega_i}. \tag{8}$$

2.3.4 Defuzzification Layer

In this layer, the outcome of the fuzzy rules is applied.

$$\overline{\omega_i} f_i = \overline{\omega_i}\left(p_i x + q_i y + r_i\right). \tag{9}$$

$p_i, q_i, and r_i$ are linear variables.

2.3.5 Output Layer

This layer is calculated by summing up the outputs of previous layers.

$$\sum_i \overline{\omega_i} f_i = \frac{\sum_i \overline{\omega_i} f_i}{\sum_i \omega_i}. \tag{10}$$

2.4 Assessment of Developed Models

To examine the strengths and weaknesses of the developed models for three techniques, MLR, ANNs, and FIS., the predicted IRI values were compared with the observed values concerning the determination coefficient of (R^2), Root Mean Square Error (RMSE), and Mean Absolute Error (MAE). Thus, a higher R^2 value was considered a better fit of the development data set. The mathematical representation of the three implemented measures is shown in the following equations:

$$\boldsymbol{R}^2 = 1 - \frac{\sum_i (\boldsymbol{t_i} - \boldsymbol{o_i})^2}{\sum_i (\boldsymbol{o_i})^2}, \tag{11}$$

$$MAE = \frac{1}{\boldsymbol{n}} \sum_{\boldsymbol{i}}^{\boldsymbol{n}} |\boldsymbol{t_i} - \boldsymbol{o_i}|, \tag{12}$$

$$RMSE = \sqrt{\frac{\sum_i (\boldsymbol{t_i} - \boldsymbol{o_i})^2}{\boldsymbol{n}}}, \tag{13}$$

where: o_i is the actual value observation I, t_i is the predicted value of observation I, n is the number of observations.

2.5 Research Goal and Methodology

This study focuses on the modelling and evaluation of roughness in flexible pavements based on pavement distress. This study aims to develop a new technique for replacing the conventional methods of determining IRI values. These include determining the IRI of flexible pavement and establishing credible prediction models for St. John's roads based on data gathered over the last few years. The IRI values were measured using a smartphone application called "TotalPave."

In this paper, the authors propose techniques based on MLR, ANN for predicting the IRI values based on pavement distress. Models named FIS were used to compare with MLR and ANN models. In detail, with data obtained from the field survey, the authors have divided the work into five phases, as follows:

- Collection of the pavement distress parameters for 19 roads (37 sections),
- Analysis of data by using the MLR technique,
- Analysis of data by using the ANN technique,
- Analysis of data by using the FIS technique, and
- Comparison and validation of the FIS, MLR, and ANNs models.

Eight pavement distress variables were studied: rutting, fatigue cracking, block cracking, longitudinal cracking, transverse cracking, potholes, patching, and delamination.

3 Study Area Location and Data Collection

The city of St. John's has a road network of more than 1000 kms of paved road. These roads are critical for the quick and safe flow of products and people in and out of St. John's.

The data collected on St. John's roads used IRI to assess pavement performance based on pavement distress. The information gathered aids in the development of models that anticipate pavement conditions. To develop flexible pavement performance and meet the goals of this research, researchers conducted a complete field investigation of pavement conditions for different roadways. The surveys covered 19 roads (37 sections) in St. John's (wet freeze climate), with pavement conditions ranging from very poor to very good in the selected sections. The survey was conducted for asphalt concrete pavement types. In this research, approximately 58 km of road length was studied, including nine significant roads (36.2 km), eight minor roads (13.5 km), and one highway (8.6 km). A smartphone application called "TotalPave" was used to collect IRI data. This program can

detect vertical movement caused by the road's rough surface and calculate the IRI value. The key motive for using this programme in the study was its property of requiring no pre- or post-processing for the pavement distress data gathered. Furthermore, TotalPave is simple to use and has a reasonable cost. The TotalPave app was installed on a smartphone and then put on the vehicle's windshield using a mobile phone holder to collect IRI data. The phone was confirmed to have experienced some bumping and vibration. The vehicle was driven at a speed of 20–80 km/h throughout data collection, according to TotalPave user instructions. Table 2 provides a descriptive summary of the St. John's road network chosen for this study for 2018 and 2021. Table 3 illustrates sample data of eight distress parameters (Fig. 3).

Ali et al. performed a distress survey on some road sections in St. John's, which was published at the 2021 Journal of Transportation Engineering, Part B: Pavements. They also studied some roads other than the sections considered in the current analysis, and the survey was presented at the 2018 Conference of the Canadian Society for Civil Engineering (CSCE) ([41, 42]. Figure 4 shows example photographs of some of the city's roads.

3.1 MLR Model Development

A MLR was used to determine the relationship between pavement distress parameters and the asphalt pavement performance index (IRI). This study developed two prediction models using the MLR technique from the collected data.

Table 3 Sample data of pavement distress

Type of distress	Unit	Elizabeth Ave Road (Section: I)		Elizabeth Ave Road (Section: II)	
		Quantity	IRI	Quantity	IRI
Rutting	(m^2)	4.80	5.3	4.4	6.02
Fatigue cracking	(m^2)	2		1.5	
Block cracking	(m^2)	0		0	
Longitudinal cracking	(m^2)	26		47.5	
Transverse cracking	(m^2)	0		0	
Patching	Number	5		7	
Potholes	(m^2)	118		96	
Delamination	(m^2)	18		13.5	

IBM's SPSS Statistics package (IBM 27) was used to analyze the data of 19 roads (37 sections) from the field survey data. Equation (14) shows a basic formula for the prediction models to find the influence of pavement distress parameters for IRI.

$$\mathrm{IRI} = \mathrm{C} + a_1X_1 + a_2X_2 + a_3X_3 + a_4X_4 + a_5X_5 + a_6X_6 + a_7X_7 + a_8X_8, \tag{14}$$

where IRI is the International Roughness Index, C is the constant, X_1 is the rutting, X_2 is the fatigue, X_3 is the block cracking, X_4 is the longitudinal cracking, X_5 is the transverse cracking, X_6 is the patching, X_7 is the potholes, X_8 is the delamination, and $a_1, a_2, a_3 \ldots\ldots\ldots\ldots a_9$ are the coefficients.

Table 2 Details of study section

Road name	Geometric type	Starting coordinate	Ending coordinate	Length (m)	IRI (2018)	IRI (2021)
Trans-Canada Highway	Highway	47.613080, −52.693132	47.572898, −52.778936	8600	1.09	1.10
Prince Philip Dr	Urban (divided)	47.588916, −52.720251	47.561888, −52.749006	3900	2.22	2.44
Portugal Cove Rd		47.595724, −52.726608	47.609546, −52.765798	3800	1.77	1.88
Elizabeth Ave Rd	Urban (undivided)	47.563756, −52.739265	47.586281, −52.708537	3500	5.3	6.02
Kenmount Rd		47.563756, −52.739265	47.586281, −52.708537	3500	2.59	3.10
Torbay Rd		47.560475, −52.749060	47.533357, −52.831811	7000	3.04	3.29
Blackhead Rd		47.599852, −52.711999	47.638361, −52.724715	4500	2.13	2.53
Logy Bay Rd		47.598178, −52.698031	47.581270, −52.704083	2000	3.98	5.83
Kenna's Hill		47.580354, −52.704381	47.571455, −52.701725	1000	4.28	3.94
Water St		47.570864, −52.697512	47.562220, −52.709403	1300	3.63	2.25
King's Bridge Rd		47.577570, −52.703921	47.571912, −52.701928	1000	5.68	4.37
Newfoundland Dr		47.539661, −52.712965	47.522431, −52.660019	8200	3.89	3.42
Newtown Rd		47.595526, −52.725829	47.591908, −52.687005	3600	4.39	4.78
Freshwater Rd		47.569411, −52.731490	47.566484, −52.716049	1300	3.50	4.26
MacDonald Dr		47.563767, −52.717459	47.561518, −52.745447	2200	2.16	2.77
Aberdeen Ave		47.590916, −52.718891	47.593944, −52.701323	1400	2.11	2.80
Empire Ave		47.619806, −52.718596	47.612738, −52.711725	1000	4.05	4.10
The Blvd		47.572286, −52.713828	47.565904, −52.729028	1400	3.19	3.87
Highland Dr		47.577727, −52.703588	47.584444, −52.684521	1600	2.94	2.59

Fig. 3 Map of the road network of the St. John's

The IRI regression models are presented in Eqs. (15) and (16), which consider eight surface pavement distresses: rutting, fatigue cracking, block cracking, longitudinal cracking, transverse cracking, potholes, patching, and delamination, as input variables and IRI output variables.

- **MLR (2018)**

Table 4 shows two IRI regression models developed based on surface pavement distress data. Rutting, fatigue cracking, block cracking, transverse cracking, and potholes have been adversely correlated with the $\mathbf{IRI}_{2018}$ model. Longitudinal cracking, patching, and delamination have been positively correlated with the $\mathbf{IRI}_{2018}$ model. The association between IRI and surface pavement distress was described as follows in Eq. (15):

$$\boldsymbol{IRI}_{2018} = 3.58 - 0.06\times_1 - 0.12\times_2 - 0.03\times_3 + 0.03\times_4 - 0.02\times_5 + 0.01\times_6 - 0.01\times_7 + 0.08\times_8. \quad (15)$$

The correlation coefficient (R^2) of this relationship is **39%.**

- **MLR (2021)**

$\boldsymbol{IRI}_{2021}$ model has been negatively correlated with rutting, block cracking, longitudinal cracking, patching, and potholes. Fatigue cracking, transverse cracking, and delamination have been positively is associated with the $\boldsymbol{IRI}_{2021}$ model. The association between IRI and surface pavement distress was illustrated as follows in Eq. (16):

$$\boldsymbol{IRI}_{2021} = 4.006 - 0.078\times_1 + 0.194\times_2 - 0.222\times_3 - 0.067 \times_4 + 0.081\times_5 - 0.004\times_6 - 0.014\times_7 + 0.015\times_8. \quad (16)$$

The correlation coefficient (R^2) of this relationship is **53.2%**.

3.2 Cross-validation Evaluating Model Performance

The cross-validation technique evaluates the model's accuracy across various data. 80% of the data samples for each subgroup (as shown in Table 2) are chosen at random to create deterioration models. The remaining 20% of data samples are used to assess the precision of prediction models.

After the validation test, Table 5 illustrates the reduction in R^2, RMSE, and MAE values for all sections. Figures 5 and 6 present the errors and linear relations for (2018 and 2021).

The following conclusions can be drawn from Table 5, Figs. 5 and 6:

- **IRI (2018):** The results showed that the reduction in R^2, RMSE and MAE values is insignificant. The reductions in accuracy are 8.21%, 16.52%, and 20.17%, respectively. As a result, the MLR technique has a good ability to predict IRI models reliably.
- **IRI (2021):** The results showed that the reduction in R^2, RMSE and MAE values are insignificant. The reductions in accuracy are 12.6%, 6.36%, and 1.31%, respectively. As a result, the MLR technique has a good ability to predict IRI models reliably.

3.3 ANN Model Development

The primary goal of model development is to predict pavement performance. The models were developed using MATLAB version R2021b. To acquire the best results, three ANN architectures were investigated: A (8-8-8-8-1-1), B (8-10-10-10-1-1), and C (8-20-10-10-1-1). Each network architecture is composed of eight inputs, three hidden layers, and one output layer. The data were divided

Fig. 4 Representative photo showing different distress types in pavement sections (Image by Abdualmtalab Ali)

Table 4 IRI models based on surface pavement distress data

Model	2018				2021			
	Unstandardized coefficients		Standardized coefficients	*t*-stat	Unstandardized coefficients		Standardized coefficients	*t*-stat
	B	Std. Error	β		B	Std. Error	β	
Constant	3.58	0.69	–	5.217	4.006	0.72	–	7.437
Rutting	−0.06	0.04	−0.28	−1.35	−0.078	0.046	−0.423	–1.849
Fatigue cracking	−0.12	0.15	−0.17	−0.801	0.194	0.161	0.15	0.636
Block cracking	−0.03	0.22	−0.03	−0.152	−0.222	0.23	−0.076	–0.342
Longitudinal cracking	0.03	0.03	0.18	1.017	−0.067	0.029	−0.363	−1.851
Transverse cracking	−0.02	0.03	−0.08	−0.529	0.081	0.033	0.049	0.278
Patching	0.01	0.01	0.13	0.753	−0.004	0.006	−0.226	−1.141
Potholes	−0.01	0.04	−0.05	−0.322	−0.014	0.044	−0.166	−0.978
Delamination	0.08	0.05	0.28	1.439	0.015	0.056	0.06	0.278
R-squared (*p*-value)	0.39 (0.05)				0.532 (0.05)			

Table 5 Validation results of prediction models

Indicator	MLR			Cross-validation			Reduction % (±)		
	R^2	RMSE	MAE	R^2	RMSE	*MAE*	R^2	RMSE	*MAE*
IRI (2018)	39	1.046	0.827	35.8	1.253	1.036	−8.21	−16.52	−20.17
IRI (2021)	53.2	0.751	0.605	46.5	0.802	0.613	−12.6	−6.36	−1.31

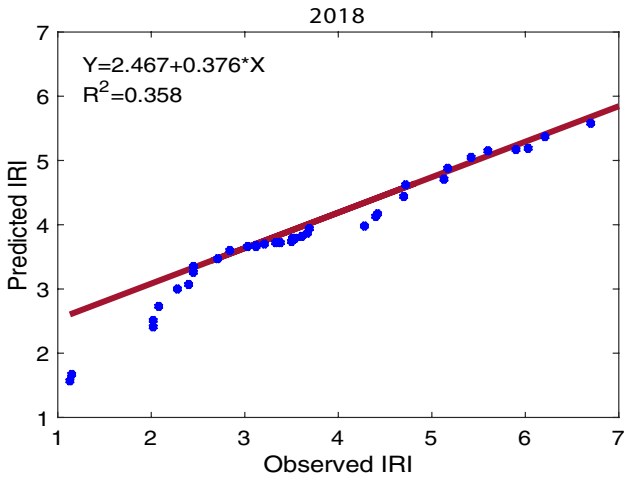

Fig. 5 Accuracy of the prediction IRI values (2018)

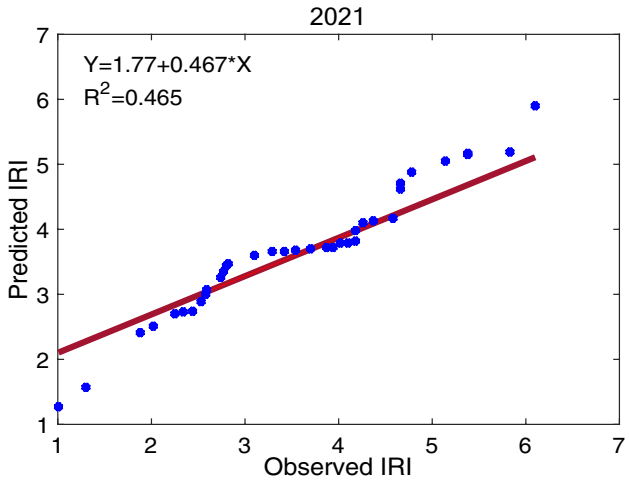

Fig. 6 Accuracy of the prediction IRI values (2021)

into three categories, 70% of the data as training, 15% of the data as testing, and 15% of the data as validation. The ANNs architecture (A), (B), and (C) are shown in Figs. 7, 8, and 9; the best results were obtained with ANN architecture (B), and the results showed a good ability of the pavement distress models. Statistical metrics such as maximum R^2 values and minimum values of (RMSE) and (MAE) contributed to selecting the best ANN network.

The findings of the ANNs approach are summarised in Table 6. The highest R^2 values were 99.2% and 99.5%, and the lowest RMSE and MAE values were (0.276), (0.234), (0.16), and (0.16) for 2018 and 2021, respectively. Figures 10 and 11 present the ANNs prediction results for IRI.

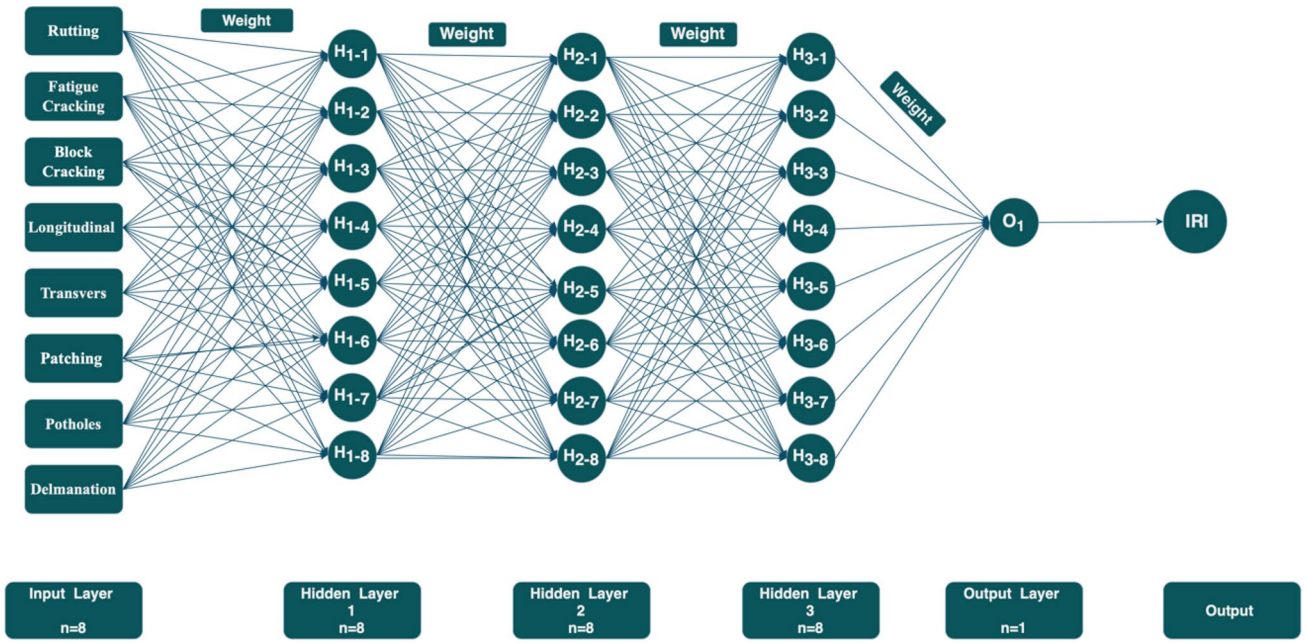

Fig. 7 Architecture of ANNs model (Model A)

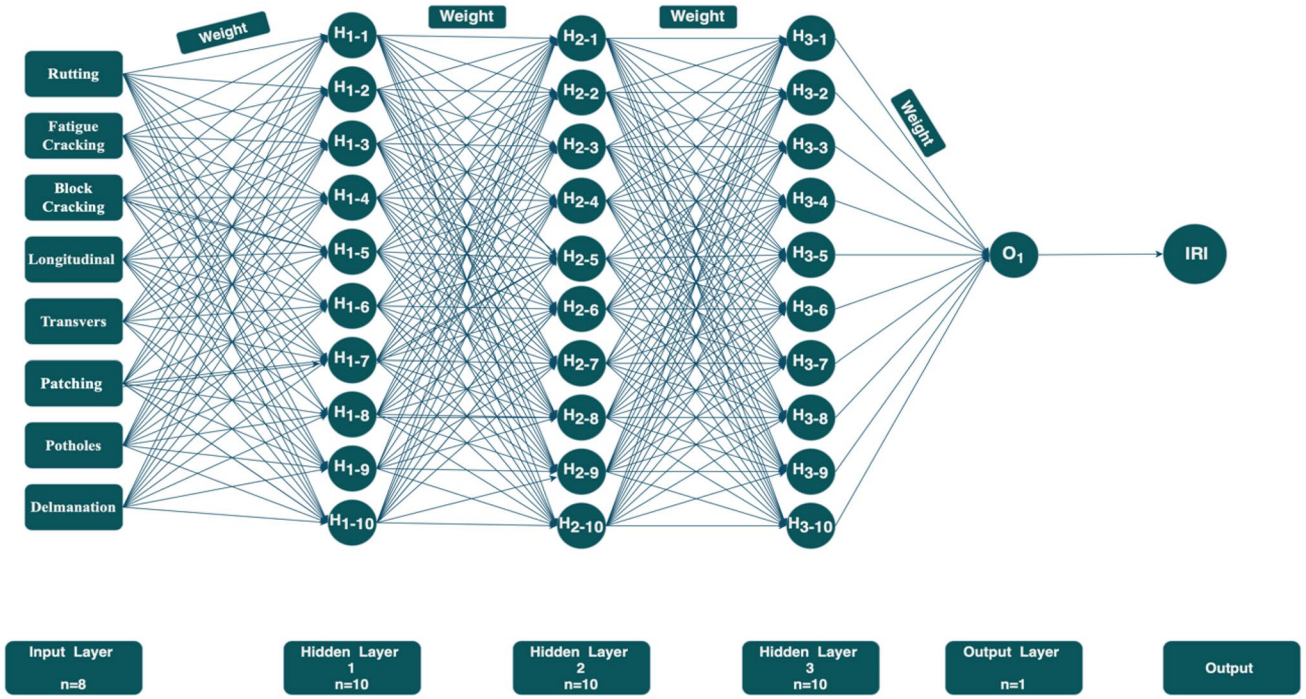

Fig. 8 Architecture of ANNs model (Model B)

3.4 FIS Model Development

The primary goal of using the FIS technique is to predict pavement performance. The models were developed using MATLAB version R2021b. The FIS technique was used on 19 roads (37 sections) in St. John's. The fuzzy model employed the severity of the degradation as the input variable to generate IRI models, while IRI was the output variable. The acquired data from the field survey were used for this. The FIS technique has three main steps,

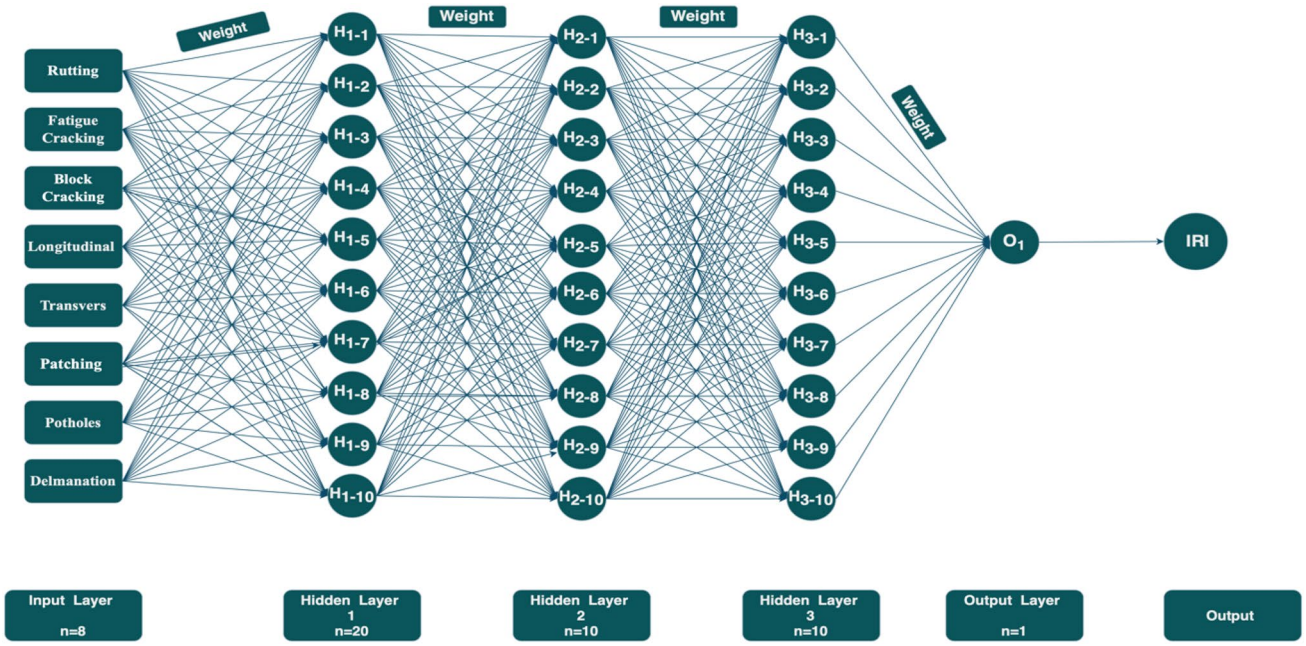

Fig. 9 Architecture of ANNs model (Model C)

Table 6 Summary of IRI models of ANNs developed

ANN model	ANNs models					
	Model (2018)			Model (2021)		
	R^2	RMSE	MAE	R^2	RMSE	MAE
8-8-8-8-1-1(A)	97.7	0.401	3.88	98.1	0.202	0.183
8-10-10-10-1-1 (B)	99.2	0.276	0.234	99.5	0.16	0.16
8-20-10-10-1-1(C)	97.8	0.349	0.339	97.1	0.279	0.225

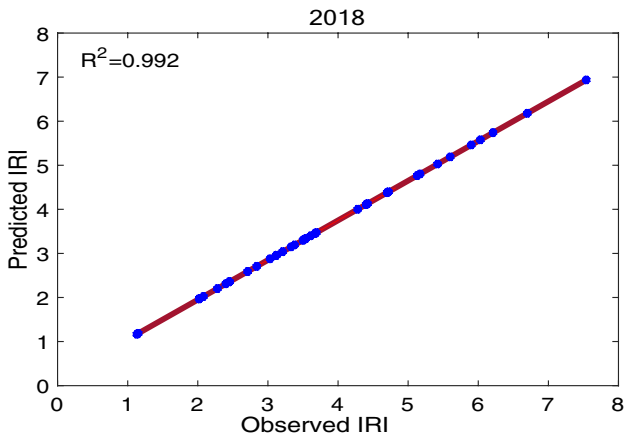

Fig. 10 ANNs model goodness-of-fit results for IRI values (2018)

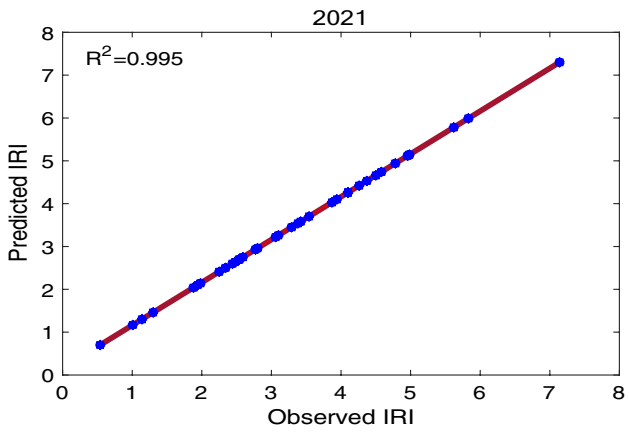

Fig. 11 ANNs model goodness-of-fit results for IRI values (2021)

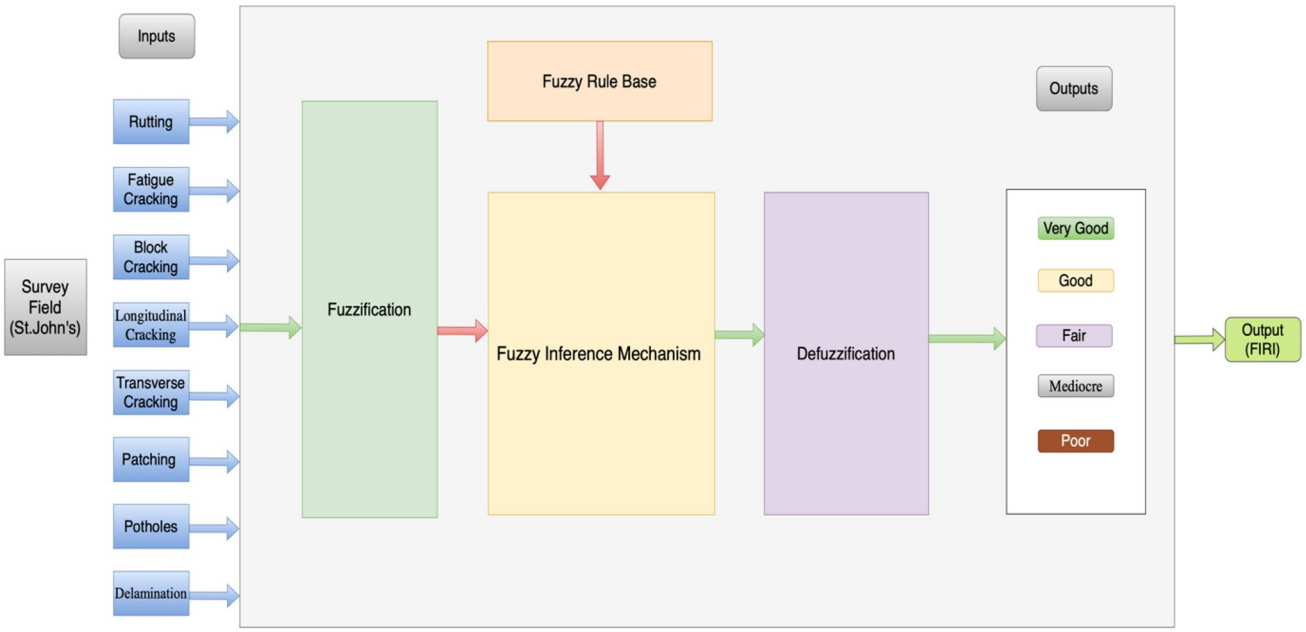

Fig. 12 Diagram of a pavement classification on FIS

the Fuzzification, Normalisation, and Defuzzification modules. Figure 12 demonstrates the main steps of the FIS technique. In the fuzzy modelling study, eight independent variables and one dependent (IRI) variable were considered inputs and outputs.

3.5 Data Pre-processing and Membership Functions

The fuzzy model was constructed with eight independent parameters based on pavement distress and one output (IRI) after collecting and revising data for 19 roads in St. John's.

All input variables' membership functions are classified as Minimal, Moderate, or Severe. The IRI membership functions for the output variables are Poor, Mediocre, Fair, Good, and Very Good. Table 7 shows pavement distress types and the number of membership functions to evaluate IRI.

3.6 Fuzzy Rule Generation

The main challenge of FIS during the second phase is developing the rules. The generation rules for the classification model described in this paper are difficult and complex, because they have eight inputs and one output. Table 8 Rule base was created for FIS and IRI.

3.7 The Results of Pavement Section Classification

The system evaluated two section datasets, each with 19 roads (37 sections), and this technique generated membership functions and rules by measuring the efficiency of fuzzy pavement classification. To display the level of agreement of

Table 7 Distress types and number of membership functions to evaluate IRI

Distress of type	Category	Number of MF	Description
Rutting	Input	Minimal, moderate, severe	Extremely important
Fatigue cracking	Input	Minimal, moderate, severe	Relatively important
Block cracking	Input	Minimal, moderate, severe	Important
Longitudinal cracking	Input	Minimal, moderate, severe	Important
Transverse cracking	Input	Minimal, moderate, severe	Moderately important
Patching	Input	Minimal, moderate, severe	Moderately important
Potholes	Input	Minimal, moderate, severe	Relatively important
Delamination	Input	Minimal, moderate, severe	Relatively important
IRI	Output	Poor, mediocre, fair, good, very good	Extremely important

Table 8 Fuzzy rules for IRI by 19 road (37 sections)

Rule no.	Distress type (Input)								IRI (Output)
	Rutting	Fatigue cracking	Block cracking	Longi-tudinal cracking	Transverse cracking	Patching	Potholes	Delamination	
1	Minimal	Minimal	Minimal	Minimal	Minimal	Minimal	Minimal	Minimal	Very Good
2	Minimal	Minimal	Minimal	Minimal	Severe	Minimal	Minimal	Minimal	Very Good
3	Minimal	Minimal	Minimal	Minimal	Moderate	Minimal	Minimal	Minimal	Very Good
4	Moderate	Moderate	Minimal	Minimal	Minimal	Minimal	Minimal	Minimal	Good
5	Minimal	Minimal	Minimal	Minimal	Moderate	Minimal	Minimal	Moderate	Good
6	Moderate	Minimal	Minimal	Moderate	Minimal	Minimal	Minimal	Minimal	Fair
7	Minimal	Moderate	Minimal	Severe	Moderate	Minimal	Minimal	Minimal	Fair
8	Moderate	Minimal	Minimal	Moderate	Moderate	Minimal	Minimal	Minimal	Mediocre
9	Minimal	Minimal	Minimal	Severe	Minimal	Minimal	Minimal	Minimal	Mediocre
10	Minimal	Minimal	Minimal	Severe	Minimal	Minimal	Minimal	Minimal	Mediocre
11	Severe	Moderate	Minimal	Minimal	Moderate	Minimal	Minimal	Minimal	Poor
12	Moderate	Minimal	Minimal	Severe	Moderate	Minimal	Minimal	Moderate	Poor
13	Severe	Severe	Minimal	Severe	Severe	Minimal	Minimal	Moderate	Poor

Table 9 Assessment of various fuzzy inference systems' configurations for 19 roads (37 sections)

Inference	Year	Defuzzification	Statistical error measures			Improvement (%)		
			R^2	RMSE	MAE	R^2	RMSE	MAE
Mamdani (Triangular)	2018	Centroid	88.3*	0.567*	0.446*	–	–	–
		Bisector	88.1	0.675	0.523	–	–	–
		Lom	88.2	0.671	0.521	–	–	–
		Som	86.3	0.988	0.797	–	–	–
	2021	Centroid	88.5*	0.537*	0.409*	0.226	5.30	8.30
		Bisector	87.2	0.54	0.411	–1.02	20.0	21.41
		Lom	86.5	0.662	0.506	–1.93	1.34	2.88
		Som	87.2	0.637	0.431	1.03	35.52	45.92

*Indicates the best results for each fuzzy system in the column

the IRI values, four defuzzified methods (Centroid, Bisector, SOM, and Lom) were used to find the R^2, RMSE, and MAE. Table 9 shows the level of agreement of the IRI values using four defuzzified methods. Figures 13 and 14 depict the relationship between observed and fuzzified IRI for 37 sections.

The FIS technique developed a section classification model for flexible pavement. An IRI was considered a FIS output, and the eight pavement distresses were considered inputs. The method was then developed in two phases for two data groups. The first phase involved creating fuzzy partitions for inputs and outputs applied a clustering algorithm. The second phase involved using four defuzzified methods to generate fuzzy rules from numerical data. The results presented that the fuzzy pavement classification has good accuracy compared to IRI calculated by MLR.

The following conclusions can be drawn from the goodness of fit statistics of the 19 road (37 sections) in Table 9:

- **Centroid Method:** The statistical indicators of R^2, RMSE, and MAE for the 2021 sections improved by 0.226%, 5.30%, and 8.30%, respectively, when compared to 2018.
- **Bisector Method:** The statistical indicators of RMSE and MAE for the 2021 sections improved by 20% and 21.41%, respectively, compared to 2018, while R^2 is decreased by 1.02% for 2021 compared to 2018.
- **Lom Method:** The statistical indicators of RMSE and MAE for the 2021 sections improved by 1.34% and 2.88%, respectively, compared to 2018, while R^2 decreased by 1.93% for 2021, compared to 2018.
- **Som Method:** The statistical indicators of R^2, RMSE, and MAE for the 2021 sections improved by 1.03%, 35.52%, and 45.92%, respectively, compared to 2018.
- According to the results, the centroid method is more accurate for 2018 and 2021 (R^2= 88.3% and 88.5%,

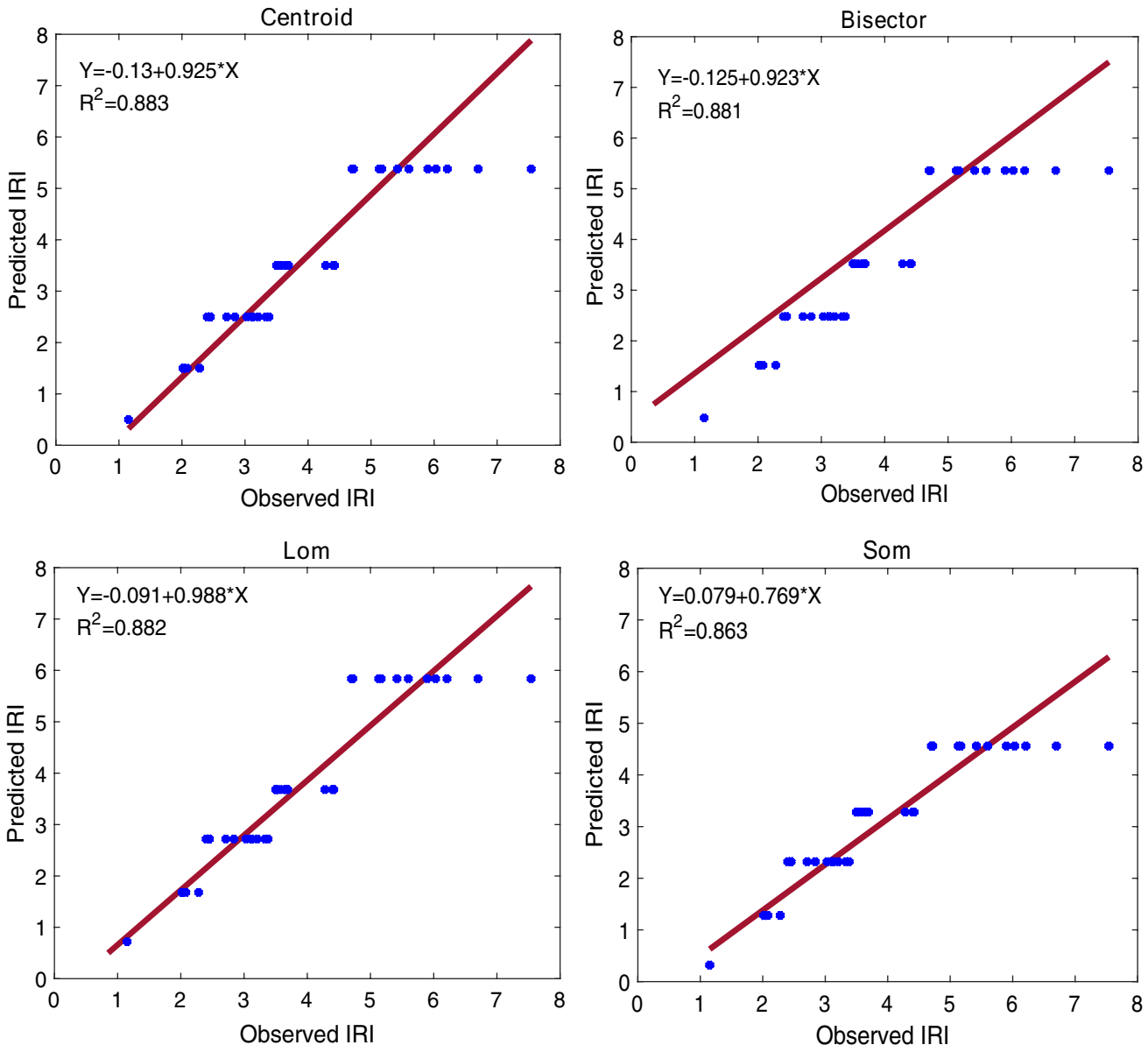

Fig. 13 Performance of a fuzzy inference system (2018)

RMSE = 0.567% and 0.537%, and MAE = 0.446% and 0.411%) than other methods.

3.8 Comparison and Validation of MLR, ANNs, and FIS Models

To validate the models developed in this study, all models were compared using MLR, FIS, and ANNs techniques. Table 10 shows that the models' performance was measured and compared using R^2, RMSE, and MAE values. Figures 15 and 16 show the comparison among the three techniques.

Several conclusions can be drawn from Table 10, and Figs. 15 and 16:

IRI (2018):

According to the statistics, the R^2 value for the ANNs model was higher than the R^2 values of the FIS and the MLR models by 10.98% and 60.7%, respectively.

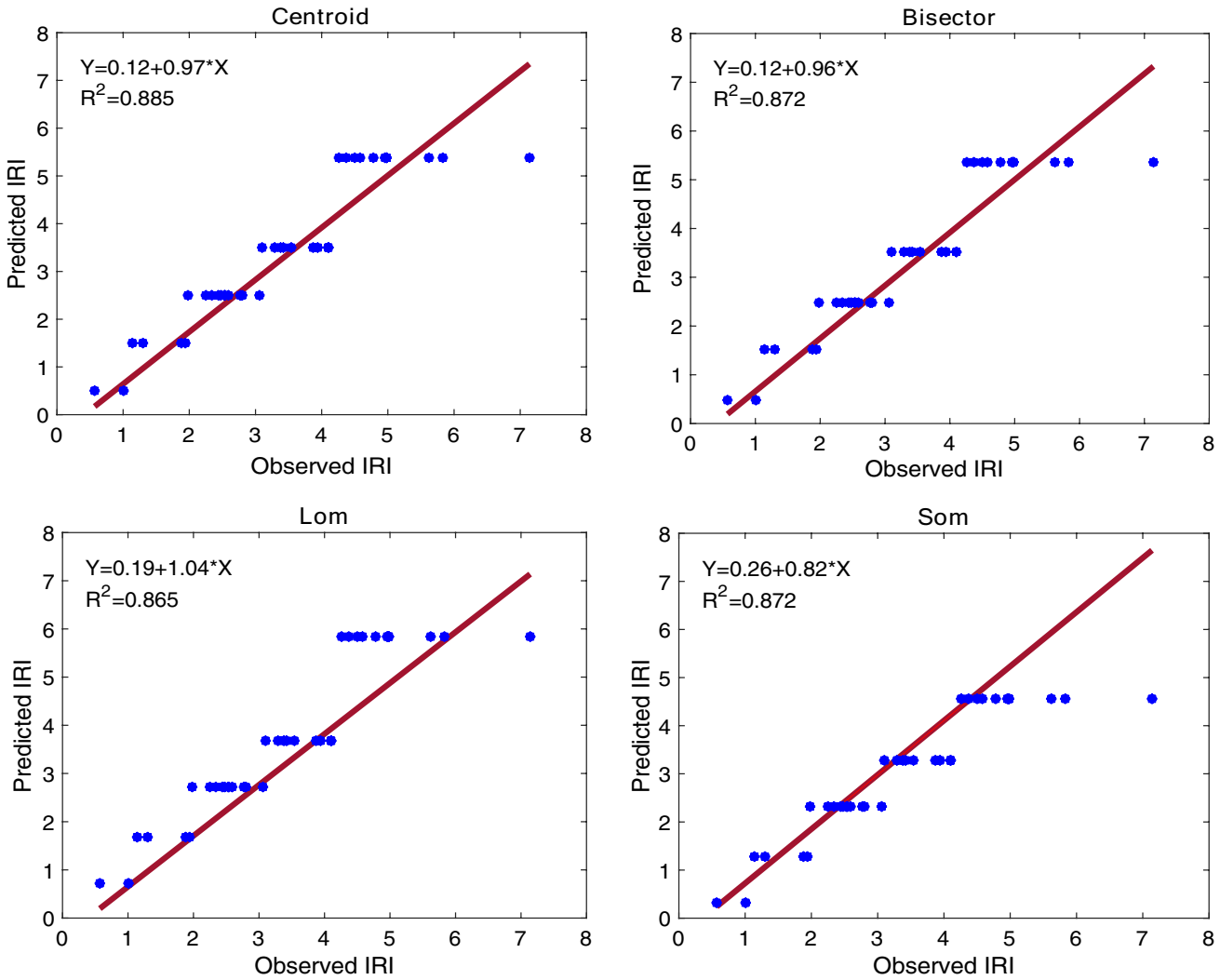

Fig. 14 Performance of a fuzzy inference system (2021)

Table 10 Comparison among MLR, FIS, and ANNs models

Technique	Year					
	2018			2021		
	R^2	RMSE	MAE	R^2	RMSE	*MAE*
MLR generated	39	1.046	0.827	53.2	0.751	0.605
FIS generated	88.3	0.567	0.446	88.5	0.54	0.411
ANNs generated	99.2	0.276	0.234	99.5	0.16	0.16

The RMSE value of the ANNs model was less than the RMSE values of the FIS and MLR models by 51.32% and 73.6%, respectively.

The MAE value of the ANNs model was less than the MAE values of the FIS and MLR models by 47.5% and 71.7%, respectively.

Fig. 15 Fitness of MLR, FIS, and ANNs models to IRI prediction (2018)

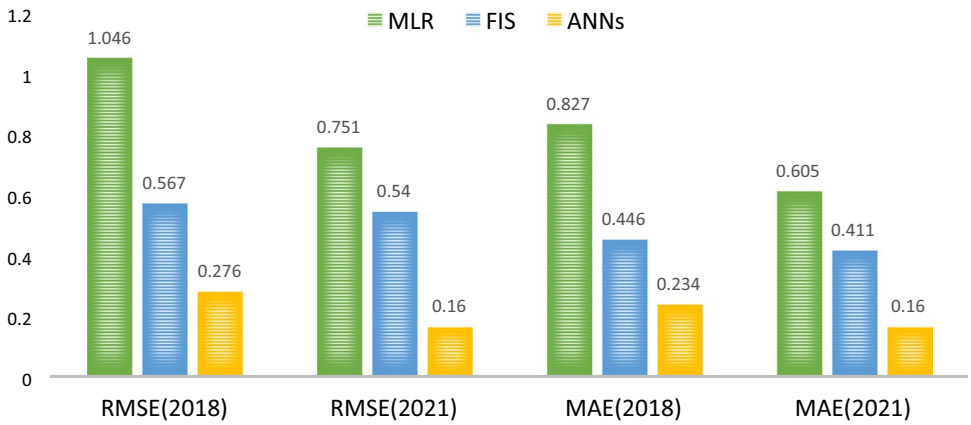

Fig. 16 Fitness of MLR and ANNs models to IRI prediction (2021)

Table 11 Sensitivity analysis of prediction models

Parameters	(R^2)	
	2018	2021
Rutting	17.4	5.4
Fatigue cracking	13.3	10
Block cracking	3.3	1.7
Longitudinal cracking	13.7	11.7
Transverse cracking	–	0.1
Patching	11.0	3.2
Potholes	0.1	0.8
Delamination	12.9	5.4

IRI (2021):
According to the statistics, the R^2 value of the ANNs model was higher than the R^2 values of the FIS and the MLR models by 46.5% and 11.01%, respectively.

The RMSE value of the ANNs model was less than the RMSE values of the FIS and MLR models by 70.4% and 78.7%, respectively.
The MAE value of the ANNs model was less than the MAE values of the FIS and MLR models by 61.1% and 73.6%, respectively.

3.9 Model Sensitivity Analysis

A sensitivity analysis was performed to investigate the effect of input variables on the efficiency of prediction IRI models. A sensitivity analysis was conducted by creating prediction models that considered each individual input while ignoring the effect of other factors. The results of the sensitivity analysis presented in Table 11, and Fig. 17 were as follows:

IRI (2018): Rutting has the most effect on the prediction model when compared to other variables. Fatigue cracking, longitudinal cracking, patching, and delamination have some

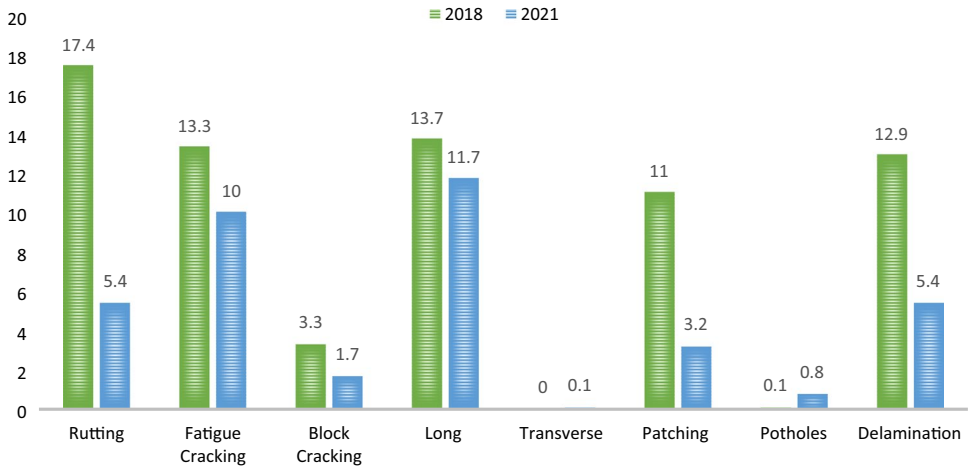

Fig. 17 Results of the sensitivity analysis of MLR (2018 and 2021)

Table 12 Chi-Square fit goodness test for St. John's

Technique	2018 X^2	2021 X^2	X^2 critical
FIS	0.017	0.020	2.722
ANN	0.001	0.004	2.722

influences on the IRI model, whereas block cracking and potholes have minor effects.

IRI (2021): Longitudinal and fatigue cracking had the most effect on the prediction model compared to other variables. Rutting, block cracking, patching, and delamination have some influences on the IRI model, while transverse cracking and potholes have minor effects.

3.10 Chi-Square Goodness of Fit Test

A chi-square goodness of fit test was performed for St. John's 19 roads (37 sections). The goodness of fit measures summarises the difference between measured and predicted values. A goodness of fit between observed and predicted frequencies is based on the quantity presented in the Eq. (17):

$$X^2 = \sum_{i=1}^{k} \frac{(o_i - e_i)^2}{e_i}, \tag{17}$$

where X^2 is a random value of a variable whose sampling distribution is approximated very closely by the chi-squared distribution with $\nu = k-1$ degree of freedom; and o_i and e_i are the observed and predicted frequencies, respectively.

A higher chi-square value indicates that the measured frequencies differ significantly from the predicted frequencies and that the fit is poor. If the observed and predicted frequencies are low, the chi-square value will be small, and the fit will be good. A good fit leads to the null hypothesis (H_o) being accepted, while a poor fit leads to its rejection.

Table 12 summarises the goodness of fit test analysis; the null hypothesis is accepted, because X^2 is less than its critical value with a 95% confidence level for 19 roads (37 sections).

4 Conclusions

The soft computing techniques help demonstrate the correlation between surface pavement distress and IRI. This paper aimed to evaluate the performance of MLR, ANNs, and FIS techniques predicting pavement performance. This case study investigated the relationship between the (IRI) indicator in asphalt pavements and eight independent variables, using 19 roads (37 sections) in 2018 and 2021 in St. John's, Newfoundland, Canada. With performance indicator data (IRI), eight surface pavement distress types were collected, including rutting, fatigue block cracking, longitudinal cracking, transverse cracking, potholes, patching, and delamination, with performance indicator data (IRI). The notable findings of this research are summarized below:

- Table 2 indicated that 81% and 84% of road sections were classified as poor in (2018) and (2021), respectively.
- The ANNs technique predicted the pavement roughness with more accuracy and the lowest errors considerably compared to the FIS techniques (2018 and 2021); a coefficient of determination indicated that the correlation was increased by 60.7% and 46.5%, respectively, while RMSE was reduced by 51.32% and 70.4%, respectively, MAE was decreased by 47.5% and 61.1%, respectively.
- The FIS technique predicted the pavement roughness with more accuracy and the lowest errors considerably compared to the MLR techniques (2018 and 2021); a coefficient of determination indicated that the correlation was increased by 55.83% and 39.89%, respectively, while

RMSE was reduced by 45.80% and 28.1%, respectively, MAE was decreased by 46.07% and 32.06%, respectively.
- From the sensitivity analysis, it is concluded that rutting, fatigue cracking, longitudinal cracking, patching, and delamination are having highest influences on the prediction model for (2018), longitudinal, fatigue cracking, rutting, block cracking, patching, and delamination are effects on the prediction model (2021).

Data Availability The submitted article appears all data, models, and code generated or used during the study.

Declarations

Conflict of Interest No potential conflict of interest was reported by the authors.

References

1. Suman, S. K., & Sinha, S. (2012). Pavement condition forecasting through artificial neural network modelling. *International Journal of Emerging Technology and Advanced Engineering, 2*(11), 474–478.
2. Li, S. E., & Peng, H. (2012). Strategies to minimize the fuel consumption of passenger cars during car-following scenarios. *Proceedings of the Institution of Mechanical Engineers, Part D: Journal of Automobile Engineering, 226*(3), 419–429.
3. Ozbay, K., & Laub, R. (2001). *Models for pavement deterioration using LTPD. FHWA-NJ-1999-030.* Washington: Federal Highway Administration.
4. Ziari, H., Sobhani, J., Ayoubinejad, J., & Hartmann, T. (2016). Prediction of IRI in short and long terms for flexible pavements: ANN and GMDH methods. *International Journal of Pavement Engineering, 17*(9), 776–788.
5. Islam, S., Buttlar, W. G., Aldunate, R. G., & Vavrik, W. R. (2014). Measurement of pavement roughness using android-based smartphone application. *Transportation Research Record, 2457*(1), 30–38.
6. Guisan, et al. (2000). Effect of boundary layer conductance on the response of stomata to humidity. *Plant, Cell & Environment, 8*(1), 55–57.
7. Attoh-Okine, N. O., Mensah, S., & Nawaiseh, M. (2003). A new technique for using multivariate adaptive regression splines (MARS) in pavement roughness prediction. *Proceedings of the Institute of Civil Engineers-Transport, 156*(1), 51–56.
8. Choi, J. H., Adams, T. M., & Bahia, H. U. (2004). Pavement roughness modeling using back-propagation neural networks. *Computer-Aided Civil and Infrastructure Engineering, 19*(4), 295–303.
9. Wang, K., Li, Q., Hall, K. D., et al. (2007). Experimentation with gray theory for pavement smoothness prediction. *Transportation Research Record, 1990*, 3–13.
10. Owolabi, A. O., Sadiq, O. M., & Abiola, O. S. (2012). Development of performance models for a typical flexible road pavement in Nigeria. *International Journal for Traffic and Transport Engineering, 2*(3), 178–184.
11. Khattak, M. J., Nur, M. A., Bhuyan, M. R. U. K., & Gaspard, K. (2014). International roughness index models for HMA overlay treatment of flexible and composite pavements. *International Journal of Pavement Engineering, 15*(4), 334–344.
12. Mubaraki, M. (2016). Highway subsurface assessment using pavement surface distress and roughness data. *International Journal of Pavement Research and Technology, 9*(5), 393–402.
13. Graupe, D. (2013). *Advanced series in circuits and systems: Volume 7 principles of artificial neural networks*. World Scientific Publishing Co. Ptc. Ltd.
14. Chen, C. T., Hung, C. T., Chou, C. C., Chiang, Z., & Lin, J. D. (2008). The predicted model of international roughness index for drainage asphalt pavement. In: International Conference on Intelligent Computing (pp. 937–945). Springer, Berlin, Heidelberg.
15. Hoang, N. D., & Nguyen, Q. L. (2018). Automatic recognition of asphalt pavement cracks based on image processing and machine learning approaches: a comparative study on classifier performance. *Mathematical Problems in Engineering*. https://doi.org/10.1155/2018/6290498
16. Hoang, N. D., & Nguyen, Q. L. (2019). A novel method for asphalt pavement crack classification based on image processing and machine learning. *Engineering with Computers, 35*(2), 487–498.
17. Nabipour, N., Karballaeezadeh, N., Dineva, A., Mosavi, A., Mohammadzadeh, S. D., & Shamshirband, S. (2019). Comparative analysis of machine learning models for prediction of remaining service life of flexible pavement. *Mathematics, 7*(12), 1198.
18. Ceylan, H., Bayrak, M. B., & Gopalakrishnan, K. (2014). Neural networks applications in pavement engineering: A recent survey. *International Journal of Pavement Research & Technology*, *7*(6), 434–444
19. Terzi, S. (2007). Modeling the pavement serviceability ratio of flexible highway pavements by artificial neural networks. *Construction and Building Materials, 21*(3), 590–593.
20. Kirbaßß, U., & Karasßahin, M. (2016). Performance models for hot mix asphalt pavements in rural roads. *Construction and Building Materials, 116*, 281–288.
21. Plati, C., Georgiou, P., & Papavasiliou, V. (2016). Simulating pavement structural condition using artificial neural networks. *Structure and Infrastructure Engineering, 12*(9), 1127–1136.
22. Amadore, A., Bosurgi, G., & Pellegrino, O. (2013). Identification of the most important factors in the compaction process. *Journal of Civil Engineering and Management, 19*(sup1), S116–S124.
23. Bosurgi, G., D'Andrea, A., & Pellegrino, O. (2013). What variables affect to a greater extent the driver's vision while driving? *Transport, 28*(4), 331–340.
24. Woldemariam, W., Murillo-Hoyos, J., & Labi, S. (2016). Estimating annual maintenance expenditures for infrastructure: Artificial neural network approach. *Journal of Infrastructure Systems, 22*(2), 04015025.
25. Xiao, F., Amirkhanian, S. N., Juang, C. H., Hu, S., & Shen, J. (2012). Model developments of long-term aged asphalt binders. *Construction and Building Materials, 37*, 248–256.
26. Amin, M. S. R., & Amador-Jiménez, L. E. (2016). Pavement management with dynamic traffic and artificial neural network: A case study of Montreal. *Canadian Journal of Civil Engineering, 43*(3), 241–251.
27. Marcelino, P., de Lurdes Antunes, M., Fortunato, E., & Gomes, M.C. (2019). Machine learning approach for pavement performance prediction. *International Journal of Pavement Engineering*, *22*, 341–354.
28. Vyas, V., Singh, A. P., & Srivastava, A. (2021). Prediction of asphalt pavement condition using FWD deflection basin parameters and artificial neural networks. *Road Materials and Pavement Design, 22*(12), 2748–2766.
29. Nitsche, P., Stütz, R., Kammer, M., & Maurer, P. (2014). Comparison of machine learning methods for evaluating pavement roughness based on vehicle response. *Journal of Computing in Civil Engineering, 28*(4), 04014015.

30. Younos, M. A., Abd El-Hakim, R. T., El-Badawy, S. M., & Afify, H. A. (2020). Multi-input performance prediction models for flexible pavements using LTPP database. *Innov Infrast Solut, 5*(1), 1–11.
31. Inkoom, S., Sobanjo, J., Barbu, A., & Niu, X. (2019). Pavement crack rating using machine learning frameworks: Partitioning, bootstrap forest, boosted trees, Naïve bayes, and K-Nearest neighbors. *Journal of Transportation Engineering, Part B: Pavements, 145*(3), 04019031.
32. Zhao, F., Di, S., Cao, J., & Tang, J. (2021). A novel cooperative multi-stage hyper-heuristic for combination optimization problems. *Complex System Modeling and Simulation, 1*(2), 91–108.
33. Zhao, F., Ma, R., & Wang, L. (2021). A self-learning discrete jaya algorithm for multiobjective energy-efficient distributed no-idle flow-shop scheduling problem in heterogeneous factory system. *IEEE Transactions on Cybernetics*, *52*(12), 12675–12686.
34. Huang, Y., & Moore, R. K. (1997). Roughness level probability prediction using artificial neural networks. *Transportation Research Record: Journal of the Transportation Research Board, 1592*, 89–97.
35. Demuth, H., & Beale, M. (1992). Neural network toolbox for use with MATLAB: User's guide. Mathworks, Natick, Mass.
36. Chang Albitres, C., Krugler, P., and Smith, R. (2005). A Knowledge Approach Oriented to Improved Strategic Decisions in Pavement Management Practices, in 1st Annual Inter-university Symposium of Infrastructure Management, Waterloo, Ontario, Canada.
37. Moazami, D., & Behbahani, H. (2011). Pavement Rehabilitation and maintenance prioritization of urban roads. *Using Fuzzy Logic, in Expert Systems with Applications, 38*(10), 12869–12879.
38. Jang, J., Sun, C., & Mizutani, E. (1997). *Mizutani neuro-fuzzy and soft computing*. Prentice Hall.
39. Zadeh, L. A. (1965). Fuzzy sets. *Information and Control, 8*, 338–353.
40. Manogaran, G., Varatharajan, R., & Priyan, M. K. (2018). Hybrid recommendation system for heart disease diagnosis based on multiple kernel learning with adaptive neuro-fuzzy inference system. *Multimedia Tools and Applications, 77*(4), 4379–4399.
41. Ali, A., Dhasmana, H., Hossain, K., & Hussein, A. (2021). Modeling pavement performance indices in harsh climate regions. *Journal of Transportation Engineering, Part B: Pavements, 147*(4), 04021049.
42. Ali, A., Hossain, K., Hussein, A., Swarna, S., Dhasmana, H., & Hossain, M. (2019). Towards development of PCI and IRI models for road networks in the City of St. John's. In: *Airfield and highway pavements 2019: Design, construction, condition evaluation, and management of pavements* (pp. 335–342). Reston, VA: American Society of Civil Engineers.

Abdualmtalab Abdualaziz Ali holds a Ph.D. degree in Civil and Environment engineering from the University of Memorial in Canada. He has a Master's degree in Civil and Environment engineering from the University of Le Havre in France. Mutalab works as a lecturer in civil engineering at the University of Azzaytuna (Tarhun–Libya). His research interests include pavement engineering, machine learning and deep learning.

Amgad Hussein is an associate professor and department head of civil engineering at Memorial. He has led the department of civil engineering at Memorial since 2014, and prior to the establishment of departments in the faculty, he was the discipline chair for four years. His research expertise is in the area of reinforced concrete structures. He has published 50 technical papers in peer-reviewed journals and conference proceedings.

Usama Heneash is a lecturer at Kafrelsheikh University and serves as a lecturer of highway engineering at the Civil engineering department, faculty of engineering. He is currently the Director of the Highway and asphalt laboratory at Kafrelsheikh University. Usama holds a Ph.D. from the University of Nottingham, England in 2013. Also, he worked as a Postdoctoral Research Associate at École de technologie supérieure (ETS, Montreal), Canada, from October 2016 to April 2017. U. Heneash worked as a Roads Consultant for Kafrelsheikh Governorate, Egypt, through 2015/2016. Usama has over 20 years of experience in highway engineering (pavement analysis, hot mix asphalt, pavement recycling, traffic, and testing materials).